Available online at www.sciencedirect.com

ScienceDirect

Procedia Engineering 10 (2011) 2917–2922

Engineering Procedia

ICM11

Mechanical and electrical properties of multi-walled carbon nanotubes by nano-manipulator

Hoon-Sik Jang[a], Sang Koo Jeon[a], Hak Joo Lee[b], Seung Hoon Nahm[a*]

[a]*Center for Materials Measurement, Korea Research Institute of Standards and Science,Daejeon 305-340, Korea*
[b]*Nano Mechanical Team, Korea Institute of Machinery and Materials, Daejeon 305-353, Korea*

Abstract

The mechanical and electrical properties of an individual multi walled carbon nanotubes (MWCNTs) were investigated by nano-manipulator in a scanning electron microscope. The mechanical strain was applied to the MWCNT by a tungsten tip controlled by a nano-manipulator. The MWCNTs used in this experiment were produced by arc-discharge method. The load response during the tensile test for the MWCNT was obtained using the force sensor which was typed with cantilever. The fractured area of the MWCNT was observed by transmission electron microscope after tensile test. The tensile strength of the MWCNT was about 41.01 GPa and the elastic modulus was calculated at 0.98 TPa. In addition, the contact resistance between the nanotube and the tungsten tip decreased with the addition of carbon deposition during e-beam exposure. The electrical resistance was significantly changed during the elongation process and corresponded with the nanotube strain. The strain sensitivity of a single MWCNT was calculated to be around 25.

Keywords: Carbon nanotubes, Mechanical test, Elastic modulus, strain sensitivity;

1. Introduction

Carbon nanotubes (CNTs) are considered to be one of likely candidates for mechanical applications such as mechanical sensor [1] and nano-motor [2] because of their superior mechanical properties and potential application in industries [3,4]. In order to apply CNTs in nano/micro systems, it is required to understand the mechanical properties of CNT. Accordingly, the strength of CNT has been predicted or calculated through several simulation techniques [5,6], and the mechanical properties of CNTs have been suggested and the young's modulus of CNTs was also computed by many authors [3,4].

Although the mechanical properties of CNTs have been reported by many researchers, the tensile properties of CNTs were rarely presented because it is difficult to control and manipulate the CNTs for

 doi:10.1016/j.proeng.2011.04.484

tensile test in a nanoscale. To determine the elastic modulus of CNTs after tensile test, it is need to compute the cross-section of nanotube. But, it is not easy to consider the cross section of the fractured nanotube before/after tensile test because the sampling for observation of the fractured nanotubes in a transmission electron microscope (TEM) is difficult. Here, we described the tensile properties of an individual multi-walled CNT (MWCNT) by using a nano-manipulator inside a scanning electron microscope (SEM). The linear deformation and the fracture behaviors of the MWCNT were observed in a SEM. After tensile test, the MWCNTs welded on the tungsten tip were observed by TEM and the cross section of MWCNTs was calculated by determining diameter and wall number of nanotube from the TEM. The tensile tests for an individual MWCNT were carried out in the SEM. The elastic modulus of MWCNTs with different synthesis methods were determined and compared. In addition, the response of an individual MWCNTs to mechanical strain has been conducted inside the SEM. The mechanical strain was applied to the MWCNTs by a tungsten tip controlled by a nano-manipulator. The MWCNT, having both ends attached to respective tungsten tips (W-tip), were elongated by moving the computer-controlled nano-manipulator. The linear deformation and elongation behaviors of individual MWCNTs including the measurement of the electrical resistance as a function of the straining process have been performed.

2. Experiments

To perform the tensile test for an individual the MWCNTs, we set up a nano-manipulator, a force sensor a W-tip in the SEM. The nano-manipulator (Klocke nanotechink) was mounted in the chamber of the SEM. The tensile loads of the MWCNTs were measured during the tensile test by the force sensor formed as a cantilever. The force sensor made by Klochke has a resolution of sub-nano Newton and a range of up to 1 mN. The force sensor was mounted on the nano-manipulator and was controlled by using a nano-manipulator and a personal computer.

In order to perform the tensile test for MWCNTs, we prepared the Arc-discharged MWCNTs and the MWCNTs grown with chemical vapor deposition (CVD). As shown in Fig. 1, the MWCNTs showed the different morphologies with different growth methods. The arc-discharged MWCNTs have the straight tubes and carbon particles as shown in Fig. 1a). The average diameter of the MWCNTs has a range from 3 nm to 33 nm, and the length was above 1 μm.. In the case of the MWCNTs grown with CVD, the MWCNTs have the curled tubes, as shown in Fig. 1b). The average diameter of the MWCNTs has a range from 5 nm to 150 nm, and the length was range from 1 μm to 10 μm.

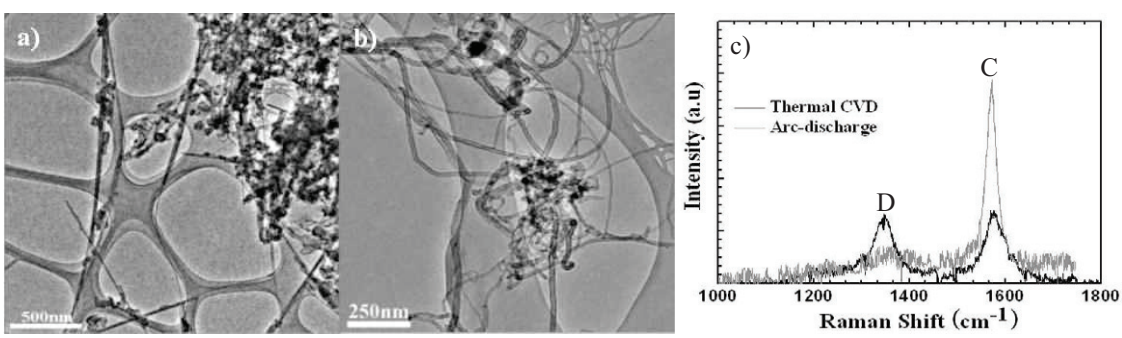

Fig. 1. TEM images of a) the arc-discharged MWCNTs and b) the MWCNTs grown with CVD. Raman results of the arc-discharged MWCNTs and the MWCNTs grown with CVD.

The Raman spactra of the MWCNTs are shown in Fig. 1c). The two main features in the Raman spectra are the D and G peaks at around 1320 and 1570 cm^{-1}, respectively, as shown in the Fig. 3. The quality of MWCNTs can be estimated as th G/D peak ratio in the Raman spectra. The G/D peak ratio of the arc-discharged MWCNTs is 1.07. In the case of the grown MWCNTs with CVD, the G/D peak ratio is 5.58. From the raman results, the quality of arc-discharged MWCNTs was better than that of the MWCNTs grown with CVD. We conformed that the MWCNTs grown with CVD have many defects as compared with the arc-discharged MWCNTs.

A nanotube was selected among the MWCNTs protruded from the heap and the MWCNT was contacted to the sensors' tip by driving the nano-manipulator. The selected MWCNT was welded on the force sensors' tip by exposing an electron-beam of the SEM. This nano-welding technique had been used to manipulate MWCNTs inside the SEM [7,8]. After the sensors' tip gripped the selected MWCNT completely, the MWCNT was detached from the MWCNTs heap by controlling the nano-manipulator. The other end of the MWCNT was attached to the W-tip by driving the nano-manipulator. Also, the end of the MWCNT was welded on the W tip by depositing carbons with E-beam. After the MWCNT was completely gripped between the tip of the force sensor and the W tip, the tensile tests for the MWCNT with different growth methods were carried out in the SEM, as shown in Fig. 2a) and b).

In order to measure the electrical resistance during the stain process of the MWCNTs, the W-tip instead of the force sensor were installed on the nano-manipulator in the SEM. One of W-tips was electrically grounded through a current meter via an electrical feedthrough. To improve the contact resistance between the nanotube and the W-tip a 5-nm-thick Au film was deposited on the W-tips by DC magnetron sputtering. The MWCNTs used in this experiment were produced by means of arc-discharge method. The MWCNT was selected the straight tube, in order to minimize the effect of unintended kinks of the MWCNT near the contacts. Two W-tips contacted both ends of the MWCNT and the contact area between the MWCNT and the W-tip was irradiated by a focused electron beam to form a better electrical and mechanical connection. The MWCNT welded on the W-tip was strained and controlled by a nano-manipulator and a personal computer (PC). The electrical resistance measurements were recorded using the PC and in-house software.

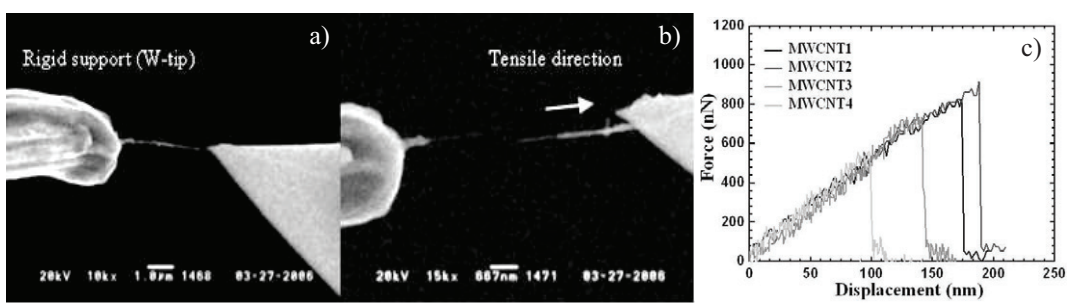

Fig. 2. SEM images of a) before and b) after tensile test of MWCNTs. c) The force-displacement curves of the MWCNTs with different growth methods during the tensile test

3. Results and discussion

The fracture behaviors of the MWCNT were successfully observed during tensile test in the SEM, as shown in Fig. 2a) and b). The force-displacement (F-D) curves of the MWCNTs with different growth methods were measured during the tensile test, as shown in Fig. 2c). The samples of the arc-discharged MWCNTs were MWCNT1 and MWCNT2, and the samples of the MWCNTs grown with CVD were MWCNT3 and MWCNT4, respectively. The tensile loads of the MWCNT1 and MWCNT2 are ~827 and

916 nN, respectively. The tensile loads of the MWCNT3 and MWCNT4 are ~755 and 557 nN, respectively. We assumed that the tensile strength of the arc-discharged MWCNTs is about 30~40 GPa. In the case of the MWCNTs grown with CVD, the tensile strength is about 10~20 GPa.

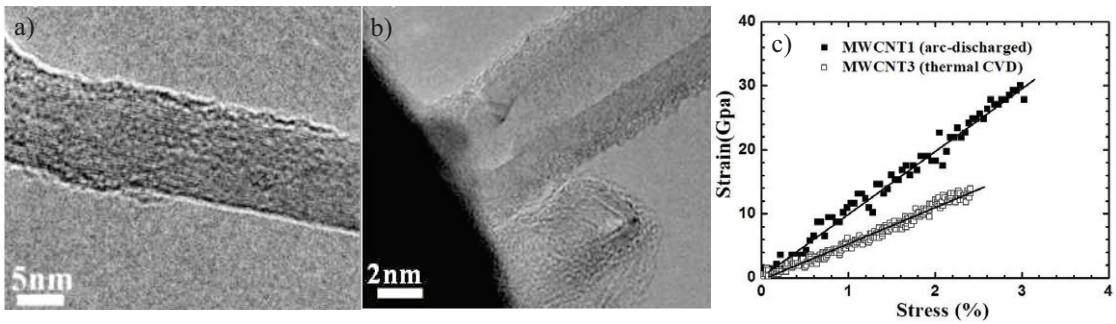

Fig. 3. TEM images of a) the arc-discharged MWCNTs (MWCNT1) and b) the MWCNTs grown with CVD (MWCNT3) gripped on the W-tip after tensile test. c) Stress-strain curve for the arc-discharged MWCNT and the grown MWCNT with CVD after tensile test.

Fig. 3 shows the TEM images of the MWCNTs gripped on the W-tip after the tensile test. Both the MWCNTs were observed the amorphous carbons on the surface of nanotubes. These carbons might be deposited during E-beam expose. In order to compute the elastic modulus of the MWCNT, we have to determine the cross-sectional area of the nanotube. The MWCNT1 and MWCNT3 gripped on the W tip were observed by TEM after the tensile test, respectively, as shown in Fig. 3a) and b). Unfortunately, the fractured area of the both of the MWCNT1 and MWCNT3 could not be imaged in high resolution mode, probably due to vibration of the nanotube. The vibrations of the tube end occurred owing to the influence of electron beam and thermal vibration [9]. However, the cross-sectional area of the MWCNTs was considered to the outer diameter and the inter diameter of the MWCNTs, and also the diameter of carbon atom and interlayer distance in nanotube were considered. Therefore, the cross-sectional area of MWCNT1 was calculated at 22.35 nm^2 and the cross-sectional area of MWCNT3 was computed at 54.18 nm^2. In order to determine the elastic modulus value, the linear region in the F-D curve shown in Fig. 2c) should then be transformed into a stress-strain curve, as shown in Fig. 3c). The ultimate tensile strength of the MWCNT1 was 41.01 GPa. The tensile elongation of the MWCNT1 at the fractured point was 4.2%. In the case of the MWCNT3, the ultimate tensile strength was 12.94 GPa and the tensile elongation at the fractured point was 2.5%.

The E value is given by the slope of a stress-strain curve: $E = \sigma / \varepsilon$, where σ is the stress and ε is the strain. The elastic modulus of MWCNT1 and MWCNT3 calculated using upside equation were ~0.98 and ~0.56 TPa, respectively. The elastic modulus of the arc-discharged MWCNTs is bigger than that of the MWCNTs grown with CVD. We assumed that this result is due to different quality of MWCNTs with different growth methods. The MWCNTs grown with CVD have more defects and disorders as compared with the arc-discharged MWCNTs. We surmised that the defects and disorders of MWCNTs induce to lower elastic modulus. However, the MWCNT is assumed to be an excellent elastic material, judging from mechanical properties such as elastic modulus and tensile strength etc.

After the individual MWCNT is completely gripped between the two W-tips, the straining process of an individual MWCNT in the direction of the tube length with the PC-driven nano-manipulator was carried out. The individual MWCNTs used in this experiment were MWCNT5 and 6 having a tube length of 4.2 and 3.9 μm and a tube diameter of 13 and 11 nm, respectively. The variation of electrical resistance is detected coincidently as a function of the straining for the individual MWCNTs as shown in Fig. 4a). To present the relationship between the electrical resistance versus strain, the variation in electrical

resistance R/R_0 was plotted against strain in Fig. 4b), where R is the current resistance and R_0 is the initial resistance. R_0 for MWCNT5 and 6 are 160 and 126 kΩ, respectively.

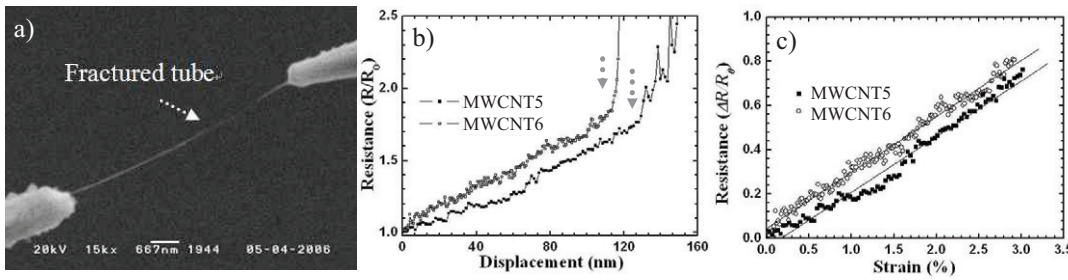

Fig. 4. a) The MWCNT fractured after straining process. b) The electrical resistance with the displacement of the tube during elongating process until the tube fracture. c) The relationship between the electrical resistance and tube strain

The electrical resistances of MWCNT5 increased linearly as MWCNT5 were elongating. MWCNT5 was fully strained and the displacement of the tube was 128 nm, just under the elastic limit. The electrical resistance was measured to be ~1.76 R_0 as MWCNT5 was fully elongated. At this time, the strain on MWCNT5 was calculated to be about 2.98%. As the straining process was continued, the resistance abruptly increased until the tube fractured. The abrupt increase in the electrical resistance denoted the irreversible physical damage to the tube. After the nanotube was perfectly fractured, the electrical resistance became infinite. Figure 4a) shows the fractured tube after the straining process. MWCNT6 was also strained the same as MWCNT5. MWCNT6 also exhibited similar behavior to MWCNT5 at full elongation as shown in Fig. 4b). The electrical resistance varied linearly with the tube displacement until the elastic limit of the nanotube was reached. The electrical resistance became infinite as the nanotube fractured. The gray dotted-arrows in Fig. 4b) indicate a border between the linear and non-linear region of the electrical resistance corresponding with the tube displacement. It was assumed that the plastic deformation and the Stone-Wales defects of a tube during elongation might not be shown in the linear region, but the plastic deformations and the Stone-Wales defects in a tube during elongation were gradually occurred in the non-linear region. The fluctuations of the electrical resistance were caused by the plastic deformations and the Stone-Wales defects of a tube, as show in the non-linear region of Fig. 4b).

Fig. 4c) shows the relationship between the electrical resistance and strain computed from the linear regions in the Fig. 4b), where ΔR is the difference between the current resistance, R, and initial resistance, R_0. From the result of the Fig. 4c), the strain sensitivity, which is one of the key performance factors for strain sensing materials, is given by $S = (\Delta R/R0)/\varepsilon$. From the slope of the fitted line in Fig. 4c), the strain sensitivity of MWCNT5 and 6 were calculated to about 25.2 and 25.9, respectively. As compared with the conventional foil gage, the strain sensitivities of MWCNT5 and 6 were much higher. They could be used for a wide strain range in strain sensing of other nano-scale materials such as tubes and wires in the near future. We also suggest that it could be applied in CNT-based mechanical sensors or devices such as force or pressure sensors.

4. Conclusion

Tensile test of an individual MWCNT was carried out using a force sensor and a nano-manipulator in the SEM. The fracture behaviors of the MWCNT were successfully observed during the tensile test in the SEM. After the tensile test, the MWCNT was observed by TEM. The elastic modulus of the arc-

discharged MWCNT and the MWCNTs grown with CVD were calculated at 0.98 and 0.56 TPa, respectively. We assumed that this result is due to different quality of MWCNTs with different growth methods. The variation of electrical resistance with the straining of a nanotube could be confirmed by *in-situ* measurement of the electrical resistance. It was also observed that the resistance of a nanotube significantly changed when the tube reached its elastic limit and failed. It could recover to its initial value of electrical resistance when strained below its elastic limit as the tube length returned to its initial value. The strain sensitivities of a MWCNT were also calculated to about 25.2 and 25.9, from the results of the relationship between the electrical resistance and strain.

Acknowledgements

This research was supported by grant (Grant No. 06K1401-00920) from the Center for Nanoscale Mechatronics & Manufacturing.

References

[1] Li CY, Chou TW. The art of writing a scientific article. *Nanotechnology* 2004;**15**:1493-6.

[2] Fenninmore AM, Yuzvinsky TD, Han WQ, Fuhrer MS, Cumings J, Zettl A. The art of writing a scientific article. *Nature* 2003;**424**:408-10.

[3] Treacy MMJ, Ebbesen TW, Gibson JM. The art of writing a scientific article. *Nature* 1996;**381**:678-80.

[4] Hernandez E, Goze C, Bernier P, Rubio A. The art of writing a scientific article. *Applied Physica A: Mateirals Science & Processing* 1999;**68**:287-92.

[5] Xin ZX, Jianjun Z, Zhong-can OY. The art of writing a scientific article. *Phys Rev B* 2000;**62**:13692-6.

[6] Liu P, Zhang YW, Lu C, Lam KY. The art of writing a scientific article. *J phys D* 2004;**37**:2358-63.

[7] Williams PH, Papadakis SJ, Falvo MR, Pate AM, Sinclair M, Seeger A, Helser A, Taylor RM, Washburn S, Superfine R. The art of writing a scientific article. *Appl Phys Lett* 2001;**80**:2547-9.

[8] Kim KS, Lim SC, Lee IB, An KH, Bae DJ, Choi S, Yoo JE, Lee YH. The art of writing a scientific article. *Rev Sci Instrum* 2003;**74**:2574-8.

[9] Jonge ND, Van Druten NJ. The art of writing a scientific article. *Ultramicroscopy* 2003;**95**:85-91.